Monthly Notices of the ROYAL ASTRONOMICAL SOCIETY

MNRAS **498,** 3730–3735 (2020) doi:10.1093/mnras/staa2517
Advance Access publication 2020 August 20

Polarimetry of the superluminous transient ASASSN-15lh

J. R. Maund [1]★ G. Leloudas,[2] D. B. Malesani [2] F. Patat,[3] J. Sollerman[4] and A. de Ugarte Postigo[5]

[1]*Department of Physics and Astronomy, University of Sheffield, Hicks Building, Hounsfield Road, Sheffield S3 7RH, UK*
[2]*DTU Space, National Space Institute, Technical University of Denmark, Elektrovej 327, DK-2800 Kgs. Lyngby, Denmark*
[3]*European Southern Observatory, Karl-Schwarzschild-Strasse 2, D-85748 Garching bei München, Germany*
[4]*Department of Astronomy, The Oskar Klein Center, Stockholm University, AlbaNova, SE-10691 Stockholm, Sweden*
[5]*Instituto de Astrofísica de Andalucía, Glorieta de la Astronomía, s/n, E-18008 Granada, Spain*

Accepted 2020 August 12. Received 2020 August 11; in original form 2020 June 1

ABSTRACT

ASASSN-15lh is the intrinsically brightest transient observed to date. Despite being the subject of concerted photometric and spectroscopic observing campaigns, there is still significant debate about the true nature of this transient and the mechanism responsible for its great luminosity. Here we report five epochs of imaging polarimetry and two epochs of spectropolarimetry conducted with the ESO Very Large Telescope (VLT) FOcal Reducer and low dispersion Spectrograph (FORS) polarimeter, spanning +28–91 d (rest frame) with respect to the light-curve maximum. The overall level of polarization across this period is seen to be low ∼0.5–0.8 per cent, however at +51.6 d, approximately corresponding to a dip in the ultraviolet (UV) photometric light curve, the polarization is seen to briefly rise to 1.2 per cent in the observed *V* band. We discuss this behaviour in the context of previous polarimetric observations of superluminous supernovae (SLSNe) and tidal disruption events (TDEs). Although the level of polarization could be consistent with polarization observed for SLSNe, the behaviour around the UV light-curve dip could also be consistent with a TDE observed almost edge on.

Key words: techniques: polarimetric – stars: black holes – supernovae: general.

1 INTRODUCTION

Polarimetry provides a unique insight into the nature of transients that is otherwise inaccessible to ordinary photometry and spectroscopy. The observed polarization properties of explosive transients, such as supernovae (SNe), provide a measure of their geometries *in the plane of the sky* at large distances, far beyond the capability of any current or planned imaging facility (for a review see Wang & Wheeler 2008). The level of polarization also provides a record of the journey of photons through the ejecta and towards us, the observers, as they interact with the exploded ejecta and with circumstellar and interstellar dust; as such, polarimetry can also potentially reveal the underlying physical processes at work in the propagation of photons.

ASASSN-15lh is intrinsically the brightest transient observed to date, reaching a peak absolute magnitude of $M_u = -23.5$ mag (Dong et al. 2016). The event was first identified by the All-Sky Automated Survey for Supernovae (ASAS-SN; Nicholls et al. 2015),[1] and subsequently determined to be exceptionally luminous (Dong et al. 2015). Based on their follow-up campaign of this object, Dong et al. (2016) concluded that this object was the most luminous ever detected superluminous supernova (SLSN) by a factor of 2. Another study by Leloudas et al. (2016), however, suggested that the luminosity of ASASSN-15lh may have arisen instead, not from the terminal explosion of a star, but from the tidal disruption [a tidal disruption event (TDE)] of a star by a rapidly spinning supermassive black hole. The true nature of ASASSN-15lh remains hotly debated, as the photometric and spectroscopic observations do not conclusively point to one specific scenario.

Here we present seven (five imaging and two spectra) epochs of polarimetric observations of ASASSN-15lh, spanning ∼28–91 d after the light-curve maximum (at MJD 57178.5; Dong et al. 2016). ASASSN-15lh was associated with the galaxy APMUKS(BJ) B215839.70–615403.9 (Nicholls et al. 2015), for which we adopt the redshift $z = 0.2326$.

2 OBSERVATIONS AND DATA REDUCTIONS

Polarimetric observations of ASASSN-15lh were conducted with the European Southern Observatory (ESO) Very Large Telescope (VLT) FOcal Reducer and low dispersion Spectrograph (FORS; Appenzeller et al. 1998). A log of the imaging and spectropolarimetric observations is presented in Table 1. The FORS instrument functions as a dual-beam spectropolarimeter and all observations used the half-wavelength retarder plate at four position angles (0°, 45°, 22.5, and 67.5) and a Wollaston prism to measure the linear Stokes parameters *Q* and *U*. The value of the degree of polarization, determined directly from the observations, may be overestimated and required a correction. We adopted the maximum probability estimator of the true polarization from Simmons & Stewart (1985), as implemented following the expression of Wang, Wheeler & Höflich (1997).

The imaging polarimetric observations (in the IPOL mode) were all conducted using the v_HIGH filter, centred on 5570 Å with an effective full width at half-maximum of 1235 Å and were reduced

★ E-mail: j.maund@sheffield.ac.uk
[1]http://www.astronomy.ohio-state.edu/asassn/index.shtml

Table 1. Log of polarimetric observations of ASASSN-15lh with VLT FORS.

Date (UT)	Phase[a] (d)	Mode[b]	Exp. time (s)
2015 July 10.26	28.2	IPOL	2 × 4 × 100
2015 July 16.30	33.1	IPOL	2 × 4 × 100
2015 July 21.29	37.1	PMOS	2 × 4 × 900
2015 Aug 08.08	51.6	IPOL	2 × 4 × 100
2015 Aug 20.39	61.6	IPOL	2 × 4 × 100
2015 Sept 2.26	72.0	IPOL	3 × 4 × 225
2015 Sept 25.13	90.6	PMOS	3 × 4 × 870

[a]Phase in rest-frame days measured with respect to the epoch of the light-curve maximum estimated by Dong et al. (2016) as 2015 June 5 (MJD 57178.5).
[b]IPOL – imaging polarimetry observation; PMOS – spectropolarimetric observation.

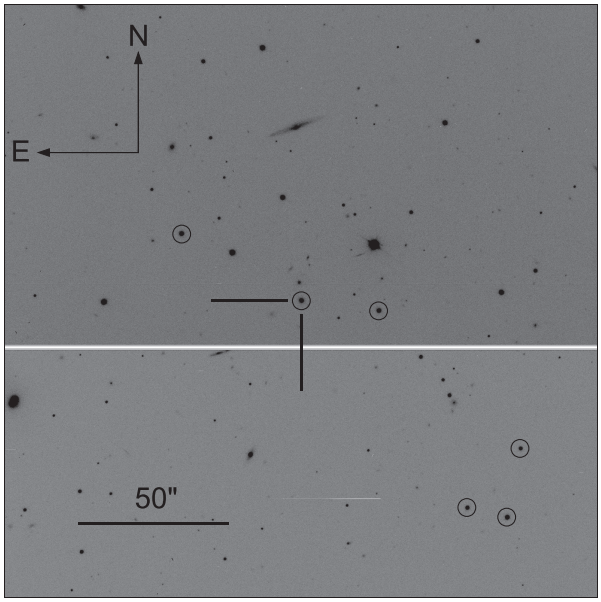

Figure 1. VLT FORS image of ASASSN-15lh using the v_HIGH filter (exposure time 5 s) on 2015 July 10. ASASSN-15lh is located at the centre of field (indicated by the cross hairs), while other sources used for photometric and polarimetric comparison are circled. The horizontal stripe across the field is the gap between the two FORS detectors.

following the prescription of Leloudas et al. (2015, see also Leloudas et al. 2017b). As FORS utilized a slitmask to prevent overlap of the ordinary and extraordinary rays, for each epoch of imaging polarimetry only one-half of the field of view of FORS was actually observed. For the FORS instrument, the instrumental polarization is negligible at the centre of the field, but increases towards the edges. For five surrounding field stars (that were available given the use of the slitmask) corrections were made for instrumental polarization as a function of position, following Patat & Romaniello (2006). The field containing ASASSN-15lh, as imaged by FORS, is shown in Fig. 1.

Spectropolarimetric observations were conducted at two separate epochs using VLT FORS (in the PMOS mode). Both sets of observations utilized the 300V grism with the GG435 order separation filter, providing a final observed wavelength coverage of ∼4500–9300 Å corresponding to a rest-frame wavelength range 3650–7545 Å. The final (rest frame) spectral resolution was 9.4 Å at 5000 Å, as measured from arc lamp calibration frames. The spectropolarimetric observations were reduced using IRAF,[2] following the prescription of Maund et al. (2007) and Patat & Romaniello (2006). The Stokes *I* spectra were flux calibrated with observations of the flux standard LTT4816 acquired on 2014 May 29, conducted with an identical instrumental set-up as the observations of ASASSN-15lh with the polarimetry optics in place. As the flux standard was not observed on the same night as the PMOS observations of ASASSN-15lh, the calibration is considered suitable for illustrative purposes only (for comparison with the linear polarization Stokes parameters). At both epochs, synthetic broad-band polarimetry was calculated using the response function for the v_HIGH filter, as used for the imaging polarimetric observations, by conducting synthetic photometry using the appropriate filter response function[3] on the individual ordinary and extraordinary ray spectra.

3 RESULTS AND ANALYSIS

3.1 Interstellar polarization

The reddening due to Galactic dust in the direction of ASASSN-15lh is limited to $E(B-V) = 0.03$ mag (Schlafly & Finkbeiner 2011). For Galactic dust, assuming a Serkowski, Mathewson & Ford (1975) relationship between polarization and reddening, the maximum expected degree of the interstellar polarization (ISP) is $p_{\rm max}$(per cent) $= 9 \times E(B-V) = 0.27$ per cent for the Galactic column and could be as much as 0.45 per cent if an additional host contribution of $E(B-V) = 0.02$ mag (Leloudas et al. 2016) is included. Following Leloudas et al. (2015), we use polarimetry derived for stars in the surrounding field (see Fig. 1) to estimate the ISP due to Galactic dust. It is important to note that, as FORS employs a series of alternating masks to prevent overlap of the ordinary and extraordinary rays on the detector, some bright stars present in Fig. 1 were not observed in the polarimetric mode. From the available sources in the surrounding field, we excluded ASASSN-15lh itself, any stars that were saturated at any epochs, and any stars with insufficient levels of signal-to-noise ratio (S/N < 300) to permit an accurate estimate of the Stokes parameters. In total, we selected five sources from the surrounding region and these are indicated in Fig. 1. We used the data at all epochs as independent measures of the Stokes parameters for each source, however we noticed significant scatter was induced if we included the data from the last epoch of IPOL observations acquired on 2015 September 2. These data were acquired 4 d after a full moon, in which the distance between the position of the moon and ASASSN-15lh on the sky was only 20°. Scattered moonlight not only increases the level of the background intensity but is polarized itself, and as such we exclude the measurements of the surrounding stars at this epoch due to enhanced levels of noise. The locations of the 20 independent measurements for the five surrounding stars are shown in Fig. 2 and all the stars appear approximately clustered in the same region in the Stokes *q*–*u* plane (where *q* and *u* are the Stokes parameters normalized for intensity *I*). Assuming these stars are all intrinsically unpolarized, we derive the weighted average foreground ISP towards ASASSN-15lh to be $q_{\rm ISP} = 0.26 \pm 0.06$ per cent and

[2]IRAF is distributed by the National Optical Astronomy Observatory, which is operated by the Association of Universities for Research in Astronomy (AURA) under a cooperative agreement with the National Science Foundation.
[3]http://www.eso.org/sci/facilities/paranal/instruments /fors/inst/Filters.html

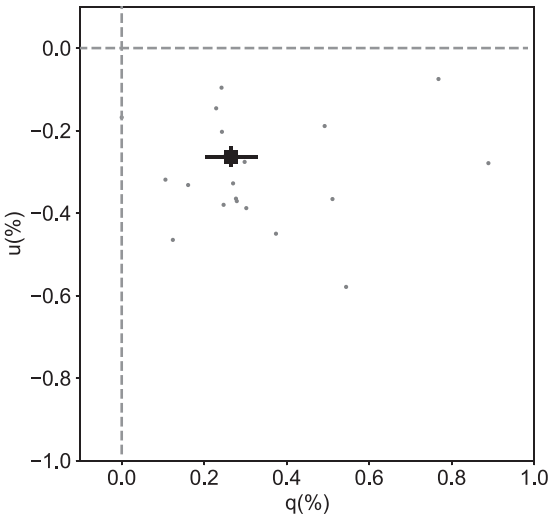

Figure 2. Measurements of the Stokes q and u parameters for five nearby stars (see Fig. 1) at four epochs (light grey) and the estimate for the ISP derived for the Galactic column of dust (■) towards to ASASSN-15lh.

$u_{\rm ISP} = -0.26 \pm 0.02$ per cent (where the quoted uncertainties are the standard error of the weighted mean), corresponding to $p_{\rm ISP} = 0.36 \pm 0.04$ per cent and $\theta_{\rm ISP} = 157\overset{\circ}{.}5 \pm 3\overset{\circ}{.}5$. The range of distances of these five stars (∼770–3695 pc; Bailer-Jones et al. 2018) and the position of ASASSN-15lh with respect to the Galactic Centre ($l = 337\overset{\circ}{.}07$, $b = -45\overset{\circ}{.}55$) suggest that this should account for all the polarization arising due to the dust along the line of sight in the Galaxy.

To ascertain if the points in Fig. 2 were consistent with independent normal distributions, in Stokes q and u, characterized by the mean and variances derived by the weighted average process, we considered the χ^2 statistic for each Stokes parameter, separately. Apart from the two measurements with $q > 0.7$ per cent, we find that the ensemble of measurements yields $\chi^2_q = 1.4$ and $\chi^2_u = 1.6$ (for 16 degrees of freedom), implying that the data are not significantly discrepant from normal distributions (Bevington & Robinson 2003).

Polarization arising from dust in the host galaxy is harder to determine. The spectropolarimetric PMOS observations of ASASSN-15lh could, potentially, provide a complete measure of the Galactic and host ISP if suitable regions of the spectrum could be assumed to be intrinsically unpolarized; however, unlike normal SNe (Wang & Wheeler 2008) and even some SLSNe (Inserra et al. 2016), there are no obvious regions of the spectrum, such as strong line emission features, in Fig. 3 that could be expected to be unpolarized. We cannot, therefore, quantify the degree of ISP arising in the host, however due to the low limit on the degree of reddening in the host, and the close proximity of ASASSN-15lh to the centre of the host (Leloudas et al. 2016), we conclude that any additional ISP is likely to be small and, while non-negligible, is unlikely to have a significant effect on our further analysis.

3.2 Spectropolarimetry

The spectropolarimetric observations of ASASSN-15lh, at 37.1 and 90.6 d, are shown in Fig. 3 (corrected for the ISP). The observation at 37.1 d has an S/N of 380 at 4100 Å, which decreases at redder wavelengths (S/N ∼ 165 at 7000 Å). The polarization spectrum at this epoch is approximately flat, with an average level of 0.5 per cent across the entire wavelength range. There are no obvious significantly polarized features in the blue portion of the spectrum and at redder wavelengths, $\lambda > 6000$ Å, the level of noise increases significantly due to strong sky lines, telluric absorption features, and fringing arising in the detector (in addition to Poisson noise). At the second epoch the overall level of polarization is approximately the same, although a possible region of enhanced polarization and depolarization is seen in the region 4250–4500 Å. The data at these wavelengths, shown in blue and cyan in Fig. 3, are clearly seen as offset from the central concentration of points on the Stokes q–u plane.

3.3 Imaging polarimetry

Imaging polarimetry of ASASSN-15lh, including synthetic polarimetry derived from the spectropolarimetric observations (see Section 3.2), is presented in Table 2. The evolution of the broadband polarization is shown in Fig. 4. Brown et al. (2016) reported a single epoch of polarimetry of ASASSN-15lh at 48.0 d (rest frame), acquired with the *Hubble Space Telescope* (*HST*) Advanced Camera for Surveys (ACS) Wide Field Channel (WFC). Using their quoted value for the approximately equivalent filter (F606W; see Fig. 3), and our values for the ISP, this polarimetry ($p = 0.45 \pm 0.06$ per cent and $\theta = 178\overset{\circ}{.}2 \pm 1\overset{\circ}{.}5$) is also plotted in Fig. 4. Brown et al. (2016) also conducted polarimetric observations using the F435W and F775W filters, reporting similar levels of polarization.

From Fig. 4, it is evident that there is a baseline level of polarization spanning the period of the polarimetric observations. Although the filter transmission functions for FORS v_HIGH and ACS/WFC F606W are not exactly identical (see Fig. 3), they cover similar wavelength ranges and the *HST* datum is consistent with the polarization measured at the immediately preceding epochs. A key exception occurs at 51.6 d, when the degree of polarization reaches 1.23 per cent. Given the uncertainties on the data, we applied at χ^2-test to derive a p-value of 0.0000162 of this being a statistical fluctuation. We have confirmed, using the polarimetric behaviour of other stars in the field and considering the instrumental signature corrections ϵ_Q and ϵ_U (Maund 2008), that there are no systematic deviations that would otherwise suggest there is a fault unique to observations at this one epoch. Interestingly, this significant increase in polarization appears correlated with the onset of significant rebrightening of ASASSN-15lh at ultraviolet (UV) wavelengths (Brown et al. 2016; Dong et al. 2016; Leloudas et al. 2016; Margutti et al. 2017).

Following this enhancement in the degree of polarization, the following epoch of 61.6 d could be interpreted as a period of 'depolarization'; however, the deviation of this measurement from the baseline is not significant, given the uncertainty on that data.

4 DISCUSSION AND CONCLUSIONS

The extreme luminosity of ASASSN-15lh has been interpreted in the contexts of both SLSNe and TDEs. Dong et al. (2016) suggested that the behaviour of ASASSN-15lh was consistent with a SLSN, although acknowledging that it was not clear which mechanism (magnetar or interaction with a dense circumstellar medium) might be responsible. The recent study by Huang & Li (2018) proposed that ASASSN-15lh could have been the explosion of a 60 $M_\odot$ star, with a large expansion velocity (∼0.02c), colliding with a dense circumstellar medium. Studies by Brown et al. (2016), Leloudas et al. (2016), and Margutti et al. (2017) have highlighted a number of key deficiencies in the interpretation of ASASSN-15lh as a SLSN, including it having occurred at the centre of a high-mass galaxy with low star formation rate unlike those associated with SLSNe

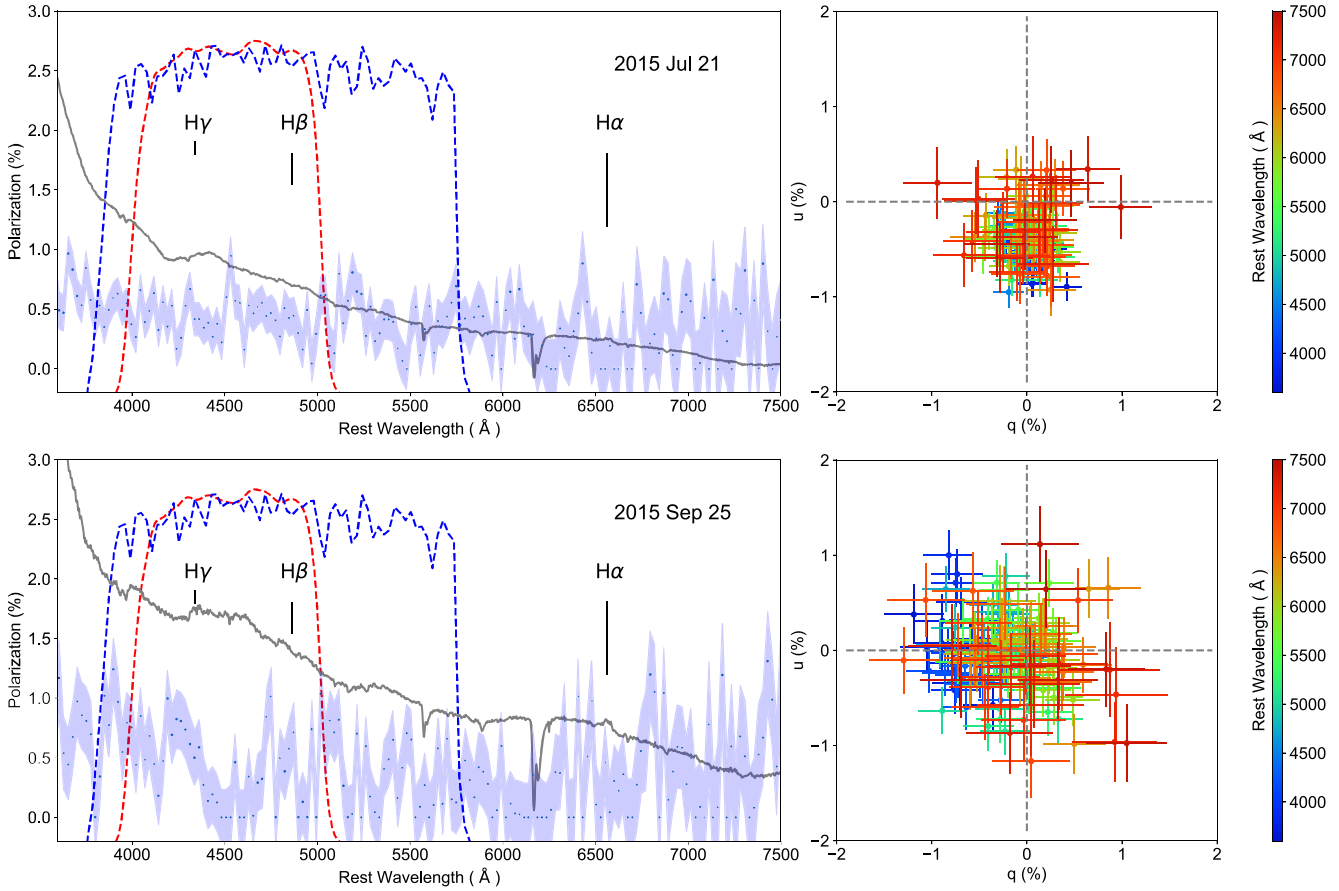

Figure 3. Spectropolarimetry of ASASSN-15lh at +37.1 d (top) and +90.6 d (bottom). Left: a comparison between the polarization (blue) and flux (grey) spectra. The transmission functions of the VLT FORS *V* band and *HST* ACS/WFC F606W filters are shown by the red and blue dashed lines, respectively. Right: the data on the Stokes *q*–*u* plane. The data have been binned to 30 Å (in the observed frame), but corrected for the redshift of the host galaxy. The data are corrected for the ISP (see Section 3.1).

Table 2. FORS polarimetry of ASASSN-15lh corrected for the interstellar polarization.

Date (UT)	Phase[a] (d)	q (%)	u (%)	p (%)	θ (°)
2015 July 10.26	28.2	− 0.48(0.33)	− 0.34(0.32)	0.40(0.33)	107.7(15.9)
2015 July 16.30	33.1	− 0.45(0.27)	0.18(0.27)	0.33(0.27)	79.4(15.9)
2015 July 21.29	37.1	0.00(0.07)	− 0.45(0.04)	0.45(0.04)	134.8(4.3)
2015 Aug 08.08	51.6	− 0.30(0.17)	− 1.21(0.14)	1.23(0.15)	127.9(4.0)
2015 Aug 20.39	61.6	0.00(0.25)	− 0.25(0.24)	0.01(0.24)	135.5(29.2)
2015 Sept 2.26	72.0	0.04(0.09)	− 0.36(0.07)	0.34(0.07)	138.3(7.5)
2015 Sept 25.13	90.6	− 0.43(0.08)	− 0.03(0.05)	0.42(0.08)	92.0(3.2)

[a]Phase in rest-frame days measured with respect to the epoch of the light-curve maximum.

but similar to the hosts of TDEs (Krühler et al. 2018), the lack of a key absorption feature at 4500 Å (usually seen in combination with the 4200 Å absorption, giving rise to the characteristic O II 'W' feature; Quimby et al. 2011), and the dip observed in the UV light curve. Observations of a later event, AT 2018fyk, which has been confirmed to be a TDE, also showed a similar dip in the UV, not replicated at other wavelengths, as seen for ASASSN-15lh (Wevers et al. 2019).

From a polarimetric perspective, the low levels of measured polarization for ASASSN-15lh are consistent with an approximately spherical structure. Following Höflich (1991), the broad-band polarization values would correspond to axial ratio >0.9, assuming an underlying spheroidal configuration. This is similar to the levels of polarization observed for SLSNe. For LSQ14mo, a Type I SLSN at a similar redshift of $z = 0.256$, Leloudas et al. (2015) reported no significant detection of polarization at five epochs (using the same instrument configuration as used here for ASASSN-15lh). Similar low degrees of polarization were also measured for the Type I SLSN 2017egm by Maund et al. (2019) in three bands covering the optical wavelength range. Alternatively, for the SLSN 2015bn, Leloudas et al. (2017a) and Inserra et al. (2016) reported increasing polarization from ∼0.54 per cent to > 1.10 per cent, with a dramatic change in the polarization properties occurring at +20 d (with respect to maximum). Inserra et al. (2016) presented two epochs

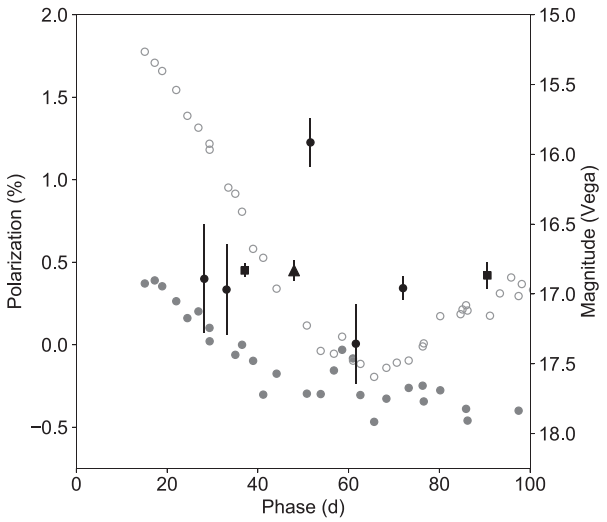

Figure 4. The broad-band ∼*V*-band polarization of ASASSN-15lh (corrected for the ISP) as a function of (rest frame) time as observed with VLT FORS in IPOL (●) and PMOS (■) modes and *HST* ACS (▲; Brown et al. 2016). Overlaid, in grey, are the *Swift* UVW1 (○) and *V*-band light curves (●) from the *Swift* Optical/Ultraviolet Supernova Archive (SOUSA; Brown et al. 2014).

of spectropolarimetry of SN 2015bn, at −24 and +24 d with respect to maximum light, showing significant evolution in the polarization between the two epochs and, importantly, clear dominant axes (Wang & Wheeler 2008) on the Stokes *q*–*u* plane (that could be explained by a mixture of continuum and line polarization). For ASASSN-15lh it is difficult to discern any polarization (in the PMOS data) associated with particular spectral features or any clear dominant axes (see Fig. 3), although there is some evolution in the polarization observed at the blue end of the spectrum. The baseline level of polarization observed for ASASSN-15lh could be consistent with the polarization previously observed for SLSNe.

The published literature for polarimetry of TDEs is limited. Wiersema et al. (2012, 2020) report high levels of polarization for Swift J164449.3+573451 ($p_K = 7.4 \pm 3.4$ per cent) and Swift J2058+0516 ($p_V = 8.1 \pm 2.5$ per cent). This high level of polarization was interpreted as arising in a relativistic jet-like outflow. Higgins et al. (2019) reported a single epoch of *V*-band polarimetry of OGLE16aaa, measuring 1.81 ± 0.42 per cent, which is of similar magnitude to the polarization measured for ASASSN-15lh by us. Lee et al. (2020) observed an evolution in the polarization of AT 2019dsg, with the degree of polarization decreasing from 9.6 ± 2.6 per cent (at 4 d after light-curve maximum) to 2.0 ± 1.0 per cent (34 d later). Rather than indicating a change in geometry, Lee et al. (2020) suggested this was due to non-thermal, relativistic emission from a jet at early times. The only spectropolarimetric observation of a TDE, reported to date, is of AT 2018dyb at a single epoch (Holoien et al. 2020). Despite the presence of broad emission lines, the polarization spectrum was flat across the optical wavelength range (at $\sim 1.5 \pm 0.5$ per cent), which suggests this polarization arose from the ISP rather than being intrinsic to the transient itself. In this regard, the lack of significant intrinsic polarization for AT 2018dyb is similar to what we have observed for ASASSN-15lh. The limited nature of these observations of other TDEs, at single epochs or limited wavelength bands, means that it is still not clear what the average level of polarization of TDEs is and what might constitute 'normal' evolution.

A key feature of the polarization of ASASSN-15lh is the sudden spike in polarization observed at 51.6 d. The lack of corroborative high polarization in measurements taken before and after this epoch could indicate this may be due to a systematic effect that we have not been able to identify. As discussed in Section 3.3, there are no peculiarities to this observation that might suggest an instrumental origin for the signal. The measured polarization uncertainties are consistent with the expected levels of S/N expected for observations with these exposure times (Patat & Romaniello 2006),[4] given the evolving brightness of ASASSN-15lh. This includes the synthetic broad-band polarization calculated from the PMOS observations. Comparison with the multiwavelength light curves of Brown et al. (2016), Leloudas et al. (2016), and Margutti et al. (2017) shows that, while the light-curve declined and rebrightened in the UV, at the wavelengths in which imaging polarimetry was conducted the light-curve evolution was relatively flat, such that the measurement was not affected by a decrease in the level of S/N at that epoch. Mummery & Balbus (2020) quantitatively model the multiwavelength light curves of ASASSN-15lh, and find it to be consistent with a 10^9 $M_\odot$ rotating black hole. The two phases of the UV light curve are found to naturally arise from this TDE model, with the rise to the second UV peak associated with the commencement of a phase dominated by emission from the accretion disc (whereas the first UV peak may come from an initial outflow). The brief spike in the level of polarization may be associated with the transition between these two different physical regimes within the TDE. If this is the case, we speculate that other TDEs, less extreme than ASASSN-15lh, might show an elevated polarization early on, supposing they are powered by accretion.

Around the time of the dip in the UV light curve, Margutti et al. (2017) also reported additional variability in the UV on time-scales of ∼5 d. If the brief increase in polarization is intrinsic to the transient, its coincidence with the dip in the UV light curve could indicate a significant change in the apparent geometric distribution of the ejecta over a time-scale of <20 d. Such variability in the polarization, over such short time-scales, has not been reported before for SLSNe; however, just as for ASASSN-15lh, polarimetric observations of SLSNe also suffer from poor cadence. Because of the 'photon hungry' nature of polarimetry (Wang & Wheeler 2008), future observing strategies may have to consider higher cadence observations to resolve possible short-term polarization fluctuations, to be better correlated with the behaviour observed in photometric light curves and spectroscopy.

The approximately spherical geometry inferred for ASASSN-15lh is consistent with the general geometric configuration of TDEs proposed by Dai et al. (2018), seen from an equatorial latitude with respect to a jet originating from the black hole. Guillochon & Ramirez-Ruiz (2015) predict that colliding streams of material may, ultimately, produce an approximately spherical geometry of material from the disrupted star. For ASASSN-15lh, therefore, the polarimetry could be interpreted as viewing this debris material and the underlying accretion disc edge on (Auchettl, Guillochon & Ramirez-Ruiz 2017; Dai et al. 2018) and obscuring a jet. This may be compared with the high polarization measured for a TDE by Wiersema et al. (2012), who concluded that they had instead seen the action of a jet, which would have required viewing the TDE from

[4] https://www.eso.org/observing/etc/bin/gen/form?INS.NAME=FORS+INS.MODE=imaging

a pole-on viewing angle. In the model proposed by Dai et al. (2018), the debris surrounding the black hole is highly ionized, and in this case the dip in the UV (also seen in another TDE, AT 2018fyk) can be explained by a change in the ionization state of this material with time, due to a change in the opacity to UV radiation (which would explain why the light-curve dip was only observed in the UV bands) as proposed by Margutti et al. (2017). The correlation of the sudden spike in polarization with the dip in the UV light curve could then correspond to, briefly, being able to see the underlying asymmetric jet and accretion disc configuration (as opposed to the opaque spherical debris material seen at other times). As noted by Leloudas et al. (2016), the dip in the light curve at UV wavelengths is also associated with a transition in the nature of the optical spectrum from being dominated by broad absorption lines to becoming almost featureless. Such dramatic changes in polarization have been observed in the case of SNe, in particular Type IIP (Leonard et al. 2006; Maund et al. 2009), coinciding with a change in the ionization properties (and optical depth) of the ejecta. The generally low polarization (except for the spike in the polarization), observed from at the latest +28 d, suggests that the overall configuration for ASASSN-15lh was approximately spherical. This implies that the debris material had already sphericalized by the time these polarimetric observations had commenced and that the emission did not, necessarily, arise from ongoing collisions between streams of material (Piran et al. 2015).

ACKNOWLEDGEMENTS

This study is based on observations collected at the European Organisation for Astronomical Research in the Southern Hemisphere under ESO programme 095.D-0633(A). The research of JRM was supported through a Royal Society University Research Fellowship. GL and DBM are supported through the Villum Fonden. AdUP acknowledges support from a Ramón y Cajal Fellowship (RyC-2012-09975).

DATA AVAILABILITY

The observational data presented here are available in the public archive of the European Southern Observatory (http://archive.eso.org) archived under programme identifier 095.D–0633(A).

REFERENCES

Appenzeller I. et al., 1998, The Messenger, 94, 1
Auchettl K., Guillochon J., Ramirez-Ruiz E., 2017, ApJ, 838, 149
Bailer-Jones C. A. L., Rybizki J., Fouesneau M., Mantelet G., Andrae R., 2018, AJ, 156, 58
Bevington P. R., Robinson D. K., 2003, Data Reduction and Error Analysis for the Physical Sciences, 3rd edn. McGraw-Hill, Boston, MA
Brown P. J., Breeveld A. A., Holland S., Kuin P., Pritchard T., 2014, Ap&SS, 354, 89
Brown P. J. et al., 2016, ApJ, 828, 3
Dai L., McKinney J. C., Roth N., Ramirez-Ruiz E., Miller M. C., 2018, ApJ, 859, L20
Dong S. et al., 2015, Astron. Telegram, 7774
Dong S. et al., 2016, Science, 351, 257
Guillochon J., Ramirez-Ruiz E., 2015, ApJ, 809, 166
Higgins A. B. et al., 2019, MNRAS, 482, 5023
Höflich P., 1991, A&A, 246, 481
Holoien T. W.-S. et al., 2020, ApJ, 898, 161
Huang Y., Li Z., 2018, ApJ, 859, 123
Inserra C., Bulla M., Sim S. A., Smartt S. J., 2016, ApJ, 831, 79
Krühler T. et al., 2018, A&A, 610, A14
Lee C.-H., Hung T., Matheson T., Soraisam M., Narayan G., Saha A., Stubens C., Wolf N., 2020, ApJ, 892, L1
Leloudas G. et al., 2015, ApJ, 815, L10
Leloudas G. et al., 2016, Nat. Astron., 1, 0002
Leloudas G. et al., 2017a, ApJ, 837, L14
Leloudas G. et al., 2017b, ApJ, 843, L17
Leonard D. C. et al., 2006, Nature, 440, 505
Margutti R. et al., 2017, ApJ, 836, 25
Maund J. R., 2008, A&A, 481, 913
Maund J., Wheeler J., Patat F., Baade D., Wang L., Höflich P., 2007, MNRAS, 381, 201
Maund J. R., Wheeler J. C., Baade D., Patat F., Höflich P., Wang L., Clocchiatti A., 2009, ApJ, 705, 1139
Maund J. R., Steele I., Jermak H., Wheeler J. C., Wiersema K., 2019, MNRAS, 482, 4057
Mummery A., Balbus S. A., 2020, MNRAS, 497, L13
Nicholls B. et al., 2015, Astron. Telegram, 7642
Patat F., Romaniello M., 2006, PASP, 118, 146
Piran T., Svirski G., Krolik J., Cheng R. M., Shiokawa H., 2015, ApJ, 806, 164
Quimby R. M. et al., 2011, Nature, 474, 487
Schlafly E. F., Finkbeiner D. P., 2011, ApJ, 737, 103
Serkowski K., Mathewson D. L., Ford V. L., 1975, ApJ, 196, 261
Simmons J. F. L., Stewart B. G., 1985, A&A, 142, 100
Wang L., Wheeler J. C., 2008, ARA&A, 46, 433
Wang L., Wheeler J. C., Höflich P., 1997, ApJ, 476, L27
Wevers T. et al., 2019, MNRAS, 488, 4816
Wiersema K. et al., 2012, MNRAS, 421, 1942
Wiersema K. et al., 2020, MNRAS, 491, 1771

This paper has been typeset from a TEX/LATEX file prepared by the author.